Journal of Materials Chemistry A

RSC Publishing

PAPER

View Article Online
View Journal | View Issue

Cite this: J. Mater. Chem. A, 2013, 1, 7415

Local probes show that framework modification in zeolites occurs on ammonium exchange without calcination†

Asel Sartbaeva,‡*[a] Nicholas H. Rees,[a] Peter P. Edwards,[a] Anibal J. Ramirez-Cuesta[b] and Emma Barney[b]

Received 16th January 2013
Accepted 25th April 2013

DOI: 10.1039/c3ta10243b

www.rsc.org/MaterialsA

Framework modification involving a change in the Al environment from tetrahedral to octahedral is frequently reported in ammonium-exchanged zeolites after calcination, steaming, acid wash and other harsh treatments. We characterized Na-Y and partially exchanged NH_4-Y zeolites by spectroscopic and diffraction methods in order to determine if NH_4 exchange itself causes framework modification. High-resolution MAS SS NMR data show that even without calcination, some Al atoms change their local environment from tetrahedral to octahedral. PDF analysis corroborates this change and shows an increase in the aluminium coordination number. TEM images show no significant change in morphology of the crystallites, and no major changes in crystallinity are detected by X-ray diffraction. A similar result is obtained on Na-A zeolite suggesting that such increase in the coordination number of Al atoms during the exchange is a common feature in zeolites. Local probes, NMR and PDF analysis show changes in the local environments of Al atoms in the framework, which are usually not possible to see in the average structure.

1 Introduction

Zeolites are highly important industrial catalysts.[1–4] Zeolites consist of a framework of corner-connected Si- and Al-tetrahedral units and extra-framework ions, which charge balance the structure ($M = Li^+$, Na^+, K^+).[5–9] The high surface area within the channels and the presence of Lewis or Brønsted acid sites make zeolites valuable catalysts. Those highly active acid sites can be created by several well known routes. Hydrothermal methods are commonly used to synthesize zeolites, after which ion-exchange is used to create NH_4^+ zeolite, which is then calcined (above 400 °C) to produce the H^+-form. It is well known that the calcination process produces acid sites, but, inevitably, it also leads to a disruption of the framework, which sometimes can result in a collapse of the zeolite framework. Here we show that even without calcination, exchange with ammonium leads to a detectable disruption of the framework, indicated by the presence of octahedral aluminium sites.

Magic Angle Spinning Solid State Nuclear Magnetic Resonance (MAS SS NMR) has been invaluable in studying the local environments of all species in zeolites since pioneering high-resolution NMR investigations on zeolites were performed by Lippmaa and co-workers in 1980s. Lippmaa *et al.*[10] reported a comprehensive study on natrolite using a high-resolution MAS SS NMR method. Since 1980s, there have been many studies reported on ^{29}Si and ^{27}Al in different zeolites and other alumino-silicates.[11–19] The ^{27}Al MAS NMR spectrum of a zeolite can contain several peaks. For most alumino-silicates, including zeolites, the relatively sharp resonance around 60 ppm corresponds to the tetrahedral aluminium species in the framework (Al^{IV}). The peak around 0 ppm has been ascribed to octahedral sites (Al^{VI}). A broad peak around 30 ppm was shown to appear as a result of a very high disruption of the framework.[11–13,16,20–24] This peak has been identified to describe highly deformed tetrahedral aluminiums, although some authors argue that this peak indicates 5-coordinated aluminiums (possibly Al^V). The latter two resonances have been shown to appear in zeolites which have been subjected to strong acid or high temperature treatments above 400 °C.

Both zeolite Y and various treated forms of zeolite Y including processes: (a) calcined above 400 °C and steamed at 700 °C;[11] (b) steamed and hydrated above 400 °C;[22] (c) treated under water vapor pressure up to 81 kPa and at a temperature of 475 °C;[21] (d) acid and temperature treated up to 650 °C[20] all show existence of octahedral aluminium sites, which manifests as a resonance around 0 ppm in the ^{27}Al MAS NMR spectrum. As these examples show high temperature treatment (above 400 °C), high temperatures steaming and acid treatment lead to the disruption of the framework and changes in the local environment of the

[a]Department of Chemistry, Inorganic Chemistry Laboratory, University of Oxford, South Parks Road, Oxford OX1 3QR, UK. E-mail: a.sartbaeva@bath.ac.uk

[b]ISIS Facility, CCLRC Rutherford Appleton Laboratory, Chilton OX11 0QX, UK

† Electronic supplementary information (ESI) available. See DOI: 10.1039/c3ta10243b

‡ Current address: Department of Chemistry, University of Bath, Claverton Down, Bath, BA2 7AY, UK.

aluminiums. There have been studies where it was possible to quantify such changes, for example, Agostini *et al.*[17] studied dealumination of zeolite Y under high temperature steaming by NMR. They attributed the formation of the peak around 30 ppm to the tetrahedral deformation and appearance of five-coordinate aluminium species. Upon heating, they showed that up to 15% of aluminium atoms adopt octahedral environment and up to 15% of aluminium atoms are in deformed tetrahedral environments or five-coordinated. Bourgeat-Lami *et al.* have shown[13] that in a previously annealed alumino-silicate framework, the change from tetrahedral to octahedral coordination of aluminium can be a reversible process, in which the Al atom does not entirely leave the framework but is coordinated by both framework oxygens and extra-framework cations.

It is clear that all mentioned treatments lead to framework modification, which is evident in changes in the Al local environment. The question we seek to address in this manuscript is whether exchange of Na^+ with ammonium without harsh thermal or chemical treatment leads to a similar framework modification.

In this study we present spectroscopic data on Na-Y and NH_4^+-Y zeolites; none of these zeolites were subjected to calcination, steaming, acid or high temperature treatments. We performed exchange of Na^+ with NH_4^+ in a zeolite Y and studied the resulting zeolites by means of high-resolution MAS SS NMR (Magic Angle Spinning Solid State Nuclear Magnetic Resonance), high-resolution TEM (Transmission Electron Microscopy), diffraction, PDF analysis (Pair-Distribution Function) and INS (Inelastic Neutron Spectroscopy) in order to determine if exchange itself leads to the disruption of the framework and changes in the local environments.

2 Experimental section

2.1 Synthesis

Synthesis of zeolite Y was modified from the recipe by Ginter *et al.*[25] In order to see if the aging of the seed gel affects the synthesis, we have prepared several samples with different aging times ranging from 1 to 30 days. We did not observe any significant difference in the resulting powders depending on the time of aging of the seed gel within that period, so we do not present data for samples with intermediate aging period. Here, we show results from four samples. For sample 1, the seed gel was aged for 1 day, and for sample 2, the gel was aged for 30 days. Details of the synthesis process can be found in the ESI.† Sample 3 was made by hydrothermal exchange (2 times of 8 hours) of sample 1 with ammonium nitrate NH_4NO_3 (Sigma-Aldrich 95 + %) at 60 °C. For the exchange, an excess of ammonium nitrate (40 g per 10 g of zeolite) was used, with ratio 40 g : 10 g : 1000 ml = NH_4NO_3 : zeolite : H_2O. Sample 4 was made by a similar exchange but with ND_4, this sample was only used for PDF analysis using neutron diffraction data collected on GEM at ISIS.

The phases were checked by X-ray diffraction (Fig. 1). Both samples 1 and 2 contained almost pure Na-Y phase with a trace amount of Na-P zeolite (less than 5%), which is a competing phase during the synthesis of FAU-type zeolites. Using program UnitCell[26] we obtained cell parameters for Na-Y = 24.7242(0.0023)Å and for NH_4-Y = 24.8128(0.0023)Å. These parameters are in good agreement with previously published data.[27–29]

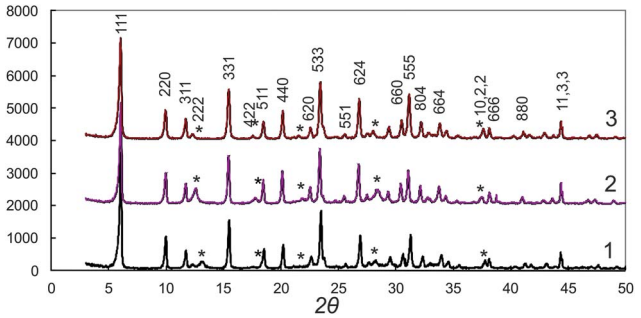

Fig. 1 X-ray diffraction patterns for three samples. Most peaks corresponding to Na-Y and NH_4^+-Y zeolites were identified, except for three peaks which are outlined by *. These can correspond to small amounts of impurities and a competing phase zeolite-P (framework type GIS).

Table 1 Elemental analysis data for three samples and Si/Al ratios calculated from elemental analysis data. These are data from averaged duplicate analysis for each element

	Si(wt%)	Al(wt%)	Na(wt%)	N(wt%)	Si/Al
1	21.17 (2.98)	10.41 (0.70)	8.72 (0.52)	—	2.03
2	16.95 (1.54)	9.48 (0.68)	7.99 (0.64)	—	1.78
3	23.66 (3.70)	11.62 (1.73)	0.79 (0.11)	4.54 (0.19)	2.02

Elemental analyses were done twice on each sample and the results in Table 1 are the averaged results from those duplicate measurements. For INS, NMR and PDF measurements all three zeolites were dehydrated at 230 °C under vacuum for 24 hours, so as to remove water molecules but not to reach calcination temperatures (usually above 400 °C) which might have induced the loss of ammonia. After dehydration all samples were handled in the glove-box to avoid adsorption on the surface.

2.2 NMR

DPMAS ^{29}Si spectra were acquired on a Varian Chemagnetics CMX Infinity 200 (4.7 T) spectrometer operating at 39.8 and 200.1 MHz for ^{29}Si and ^{1}H respectively and at a MAS rate of 4 kHz. Typically 5000 transients were acquired with an acquisition time of 68 ms (1024 data points zero filled to 16 k) and a recycle delay of 30 s. All ^{29}Si spectra were externally referenced to kaolinite (taken to be at $\delta = -91.7$ ppm on a scale where δ(TMS) = 0) as a secondary reference. Solid state ^{27}Al MAS spectra were obtained at 104.2 MHz (9.4 T) on a Varian/Chemagnetics Infinity 400 (9.4 T) spectrometer, using a sample rotation rate of 15 kHz. In order to obtain quantitative MAS spectra, a single pulse excitation was applied using a short pulse length (0.7 μs). Each spectrum resulted from 2000 scans separated by a 1 s delay. The ^{27}Al chemical shifts are referenced to an aqueous solution of $Al(NO_3)_3$ (0 ppm).

2.3 Neutron diffraction method and analysis

The neutron diffraction data were measured using the GEM diffractometer[30] at the ISIS pulsed neutron source at the

Rutherford Appleton Laboratory, UK. In order to calculate the coordination number of Al atoms, we have performed PDF analysis on two samples – sample 1 and sample 4. For these purposes sample 1 was exchanged with deuterated ammonium ND_4 to make sample 4. Vanadium cans with eight mm diameter were used to contain the samples, in the form of powder. The data were reduced and corrected for attenuation and multiple scattering, using the standard GUDRUN and ATLAS[30] software to extract the atomic pair-distribution functions (PDF). Following these corrections, the coherent scattering intensity, $i(Q)$, was identified by

$$i(Q) = \sum_i \sum_j c_i c_j b_i b_j [p_{ij}(Q) - 1] \quad (1)$$

where c_i, c_j, b_i and b_j represent the atomic concentration and coherent scattering length of the chemical species i and j respectively, and $p_{ij}(Q)$ is the pair correlation function. Fourier transformation of $i(Q)$ generates the total correlation function, $T(r)$, given by

$$T(r) = T^0(r) + \frac{2}{\pi} \int_0^\infty Qi(Q)M(Q)\sin(Qr)\, dQ \quad (2)$$

where $M(Q)$ is a Lorch window function, and $T^0(r)$ is the average density term given by:

$$T^0(r) = 4\pi r p^0 \left(\sum_i c_i b_i \right)^2 \quad (3)$$

where r is the distance from an arbitrary atom at the origin and p^0 is the number density. More detailed information on the neutron diffraction method and PDF analysis can be found elsewhere.[30,31] The composition of the ammonium containing sample used for the data analysis was based on the compositional analysis given in Table 1. Data analysis was complicated by the fact that samples contained some hydrogen. The composition used for the ND_4-Y samples was based on the elemental analysis data from Table 1.

2.4 TEM measurements

Na-Y (sample 1) and ammonium exchanged zeolite Y (sample 3) were dispersed in acetone using an ultrasound bath to form a suspension. A standard 200 mesh TEM Cu grid covered with a thin holey amorphous carbon film was dipped into the suspension and dried out in the atmosphere at room temperature. Images of the materials were obtained in a JEOL 3000F field emission gun TEM operating at 300 kV and equipped with a Gatan slow scan 1k1k pixel CCD camera. Energy dispersive X-ray analyses (EDX) were performed in the TEM to characterize the chemical composition (see ESI†).

2.5 INS measurements

Inelastic neutron scattering data were measured using the crystal-analyser inverse-geometry time of flight (ToF) spectrometer, TOSCA[32–34] at the ISIS pulsed spallation neutron source. The theory and details of the INS method can be found elsewhere.[32,35] All samples were dehydrated before INS measurements and loaded in cans in an inert atmosphere. TOSCA is an indirect geometry time-of-flight spectrometer with its optimal energy range of 0–4000 cm^{-1} (0–500 meV). We first collected a background spectrum at temperature below 20 K for both samples.

3 Results

In this section, we present data from Inelastic Neutron Scattering measurements collected on TOSCA instrument at the ISIS facility, Magic Angle Spinning Solid State NMR measurements collected at Oxford (Department of Chemistry), Pair-Distribution Function measurements collected on GEM instrument at the ISIS facility, high-resolution TEM measurements collected at Oxford (Department of Materials).

3.1 INS data

INS spectra for Na-Y and NH_4^+-Y zeolite samples at 20 K are shown in Fig. 2. These data are in good agreement with the results previously reported on Na-Y and NH_4^+-Y zeolites by Jacobs *et al.*[36] There is a visible enhancement of scattering in the NH_4^+-Y sample at energy losses around 70 meV and below, with peaks visible at around 20 meV attributable to translational modes of ammonium ions and at around 40 meV attributable to restricted librational modes.

The large incoherent scattering cross-section of hydrogen makes INS particularly sensitive to hydrogen containing molecules such as ammonium. Our previous studies have shown that even low levels of ammonium exchange in zeolites lead to visible changes in INS spectra.[37–39]

3.2 NMR data

The values of δ of the individual components of the ^{29}Si MAS NMR signal due to the resonance absorption of the Si atoms in $Si(OAl)_n(OSi)_{4-n}$ are designated for brevity as $Si(nAl)$, where n = 0, 1, 2, 3 and 4 corresponds to the number of framework Al atoms in the nearest surroundings of the particular Si atoms (Fig. 3). Those δ values and the relative values of the integral

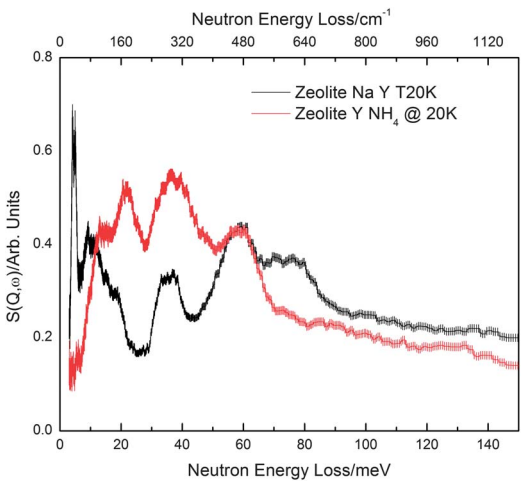

Fig. 2 INS spectra for Na-Y and NH_4^+-Y zeolites showing back scattering. Stainless steel can background has been extracted.

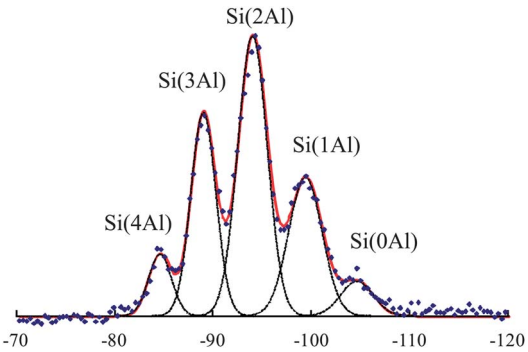

Fig. 3 High-resolution ^{29}Si MAS SS NMR spectrum for sample 1 (Na-Y) collected at 39.75 MHz. Experimental spectrum – blue symbols, red line – computer simulated spectrum, fitted with pseudo-Voigt peak profiles. Individual deconvoluted peaks are shown as black dotted lines.

intensities of the corresponding components of each signal separated from the general absorption profile assuming the pseudo-Voigt form of the individual lines are listed in Table 2.

As can be seen from Table 2, samples 1 and 2 show similar environments of Si, which is manifested in compatible δ of the individual components of the ^{29}Si signal. This is in good agreement with previously published data.[18,19,40]

As we replace Na^+ with NH_4 we see a slight increase in chemical shifts of all peaks in the signal, especially the Si(4Al). In contrast we see a considerable change in intensities of all peaks. We calculate the relative integral intensity $I_{Si(n\mathrm{Al})}$ of each peak in the ^{29}Si spectrum by normalizing to a total intensity of unity. The values of Si/Al listed in Table 2 were calculated by the formula

$$\mathrm{Si/Al} = \sum_{n=0}^{4} I_{Si(n\mathrm{Al})} \Big/ \sum_{n=0}^{4} (n/4) I_{Si(n\mathrm{Al})} \quad (4)$$

The calculation using this Si/Al ratio provides a quantitative measure of the zeolitic composition independently of the elemental chemical analysis. The deconvolution of the ^{29}Si spectrum of sample 1 leads to the ratio of intensities of the five peaks of 1.03 : 4.18 : 6.42 : 3.83 : 0.69, corresponding to (Si/Al) NMR = 2.06, in a reasonable agreement with elemental analysis (Table 1). The deconvolution of the ^{29}Si spectrum of sample 2 leads to the ratio of intensities of the five peaks of 1.47 : 3.14 : 6.28 : 3.99 : 1.08, corresponding to (Si/Al) NMR = 1.99, which is again in a reasonable agreement with elemental analysis (Table 1).

Sample 3 was exchanged with NH_4^+. The deconvolution of the ^{29}Si spectrum of sample 3 leads to the ratio of intensities of the five peaks of 1.23 : 4.01 : 6.73 : 3.32 : 0.92. Under the assumption of an uninterrupted tetrahedral framework, this corresponds to (Si/Al) NMR = 2.08, as in sample 1; however if Al ions have left the framework the true Si/Al ratio in the framework will be higher, as discussed later. Although the intensities do not show much change, the spectrum for this sample is different. It still shows three distinctive peaks corresponding to Si(1Al), Si(2Al) and Si(3Al) (Fig. 4). However, two other peaks corresponding to Si(0Al) and Si(4Al) shifted and became much broader. The fitted widths show that while widths of three peaks Si(1Al), Si(2Al) and Si(3Al) have increased in sample 3 by about 15%, the width of peak Si(4Al) has increased by more than 45%. This is reasonable as statistically this peak Si(4Al) would be affected first if aluminium ions were to leave the framework and move into the interstitial positions, which might be expected during the exchange. The presence of Si–OH groups in the framework, as a result of Al extraction, will also contribute to the peak broadening in the ^{29}Si spectrum of sample 3.

The ^{27}Al spectrum of sample 1 shows one relatively narrow signal with a chemical shift of 62.43 ppm (Fig. 5), corresponding to the tetrahedrally bound aluminium, showing that the framework is not disrupted. This is in general agreement with previously published data.[11,22–24] The ^{27}Al spectrum of sample 2 showed a similar large single signal with a chemical shift of 62.48 ppm, with no other signals. These similarities in the ratios of intensities of the ^{29}Si spectra and in chemical shifts of ^{27}Al show that there are no significant changes in the framework composition of samples 1 and 2, despite the aging of the seed gel during the preparation of the samples.

Table 2 NMR data from ^{29}Si spectra for samples 1–3: Si/Al ratios and aluminium first neighbor distributions Si(nAl) calculated from NMR data for three samples. * This calculation assumes an uninterrupted framework and the true Si/Al value for sample 3 is higher; see Fig. 5 and Table 3

		δ (ppm)				
	Si/Al (NMR)	Si(4Al)	Si(3Al)	Si(2Al)	Si(1Al)	Si(0Al)
1	2.06(3)	−84.35	−89.14	−94.30	−99.47	−104.63
2	1.99(3)	−84.52	−89.69	−94.85	−100.01	−105.18
3	2.08(3)*	−87.64	−90.90	−95.67	−100.88	−105.96

Table 3 NMR data from ^{27}Al spectra for samples 1 and 3: Si/Al ratio and chemical shifts from ^{27}Al NMR data for samples 1 and 3

Sample	Si/Al (NMR)	Tetrahedral peak δ (ppm)	Octahedral peak δ (ppm)
1	n/a	62.43	none
3	2.32	55.77	−0.85

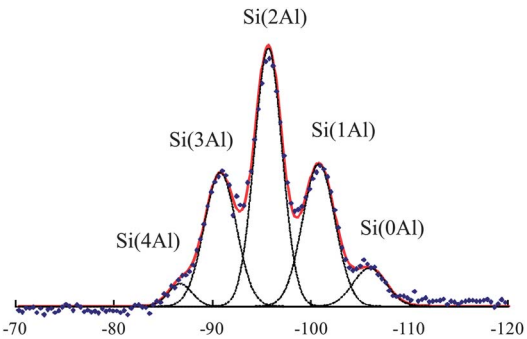

Fig. 4 High-resolution ^{29}Si MAS SS NMR spectrum for sample 3 (NH_4-Y), collected at 39.75 MHz. Experimental spectrum – blue symbols, red line – computer simulated spectrum, fitted with pseudo-Voigt peak profiles. Individual deconvoluted peaks are shown as black dotted lines.

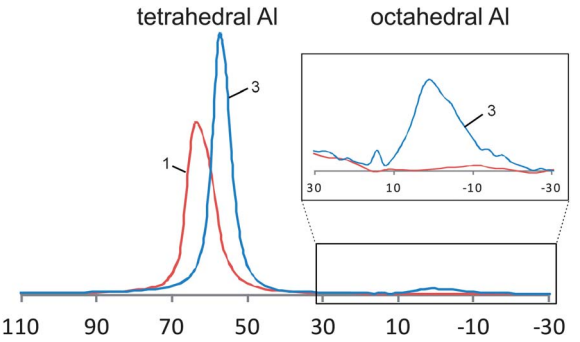

Fig. 5 High-resolution ^{27}Al MAS SS NMR spectra for sample 1 (Na-Y) in blue and sample 3 (NH_4^+-Y) in red, collected at 104.198 MHz. Peaks, centred at 62.43 ppm for sample 1 and 55.77 ppm for sample 3, correspond to tetrahedrally coordinated Al. Inset shows a peak at −0.85 ppm which corresponds to octahedral Al. No octahedral Al are observed in sample 1.

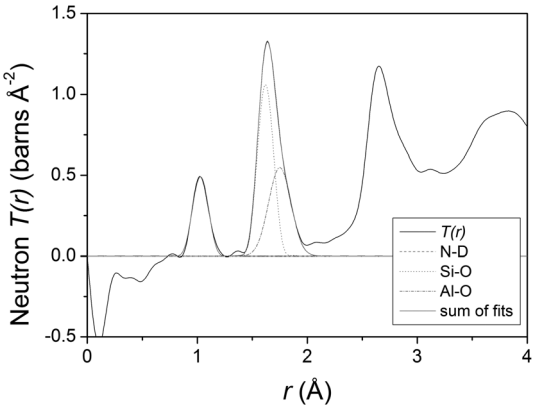

Fig. 6 $T(r)$ data for the ND_4-Y sample, with fits to the first three peaks in the correlation function.

The ^{27}Al MAS NMR spectrum of sample 3 shows two distinct signals: a large one at 56.75 ppm corresponding to aluminium still remaining in tetrahedral sites, and a smaller one at −0.52 ppm corresponding unmistakably to Al in octahedral coordination (Fig. 5). The ratio r of the intensities of the tetrahedral and the octahedral signals is 8. Both peaks were fitted with pseudo-Voigt function, which showed predominance of a Lorentzian component. Although the height of this octahedral peak is small, it is also wide, thus having a relatively large area. The total amount of aluminium atoms in samples 1 and 3 is the same, as no washing or any other treatment was performed. Thus we can calculate the Si/Al = $2.06(1 + r)/r = 2.32$ for the composition of the tetrahedral framework only. This value is higher than the 2.08 previously calculated from the ^{29}Si spectrum (Fig. 4 and Table 2), further indicating that changes in the aluminium environment have affected the ^{29}Si spectrum of sample 3 and invalidated the assumption of an uninterrupted tetrahedral framework. If we assume that all Al in a tetrahedral peak have coordination number 4 and all Al under an octahedral peak have coordination number 6, then using the convolution of those two peaks we get an average coordination number for NH_4^+-Y close to 4.19.

Since we do not observe changes in the average structure by X-ray diffraction, but only see the framework modification by a local probe such as NMR, we have also performed PDF analysis of sample 1 (Na-Y) and sample 4 (ND_4-Y) using neutron diffraction data collected on a high-resolution GEM diffractometer.

3.3 PDF data

The total correlation function, and the fit to the N–D, Si–O and Al–O peaks are given in Fig. 6. The peak position and area of the Si–O peak were fixed during the fit to ensure a coordination number of 4. This approach allows the coordination number of aluminium to be determined and compared to the results from NMR. The coordination number of the N–D peak is too low, which could indicate that the amount of nitrogen in the sample has been overestimated. However a substantial decrease in the nitrogen content would give Si–O and Al–O coordination numbers which are too low. A more likely explanation for the poor agreement between the expected and measured N–D coordination number is the presence of hydrogen. H has a negative scattering length while D has a positive scattering length, and so the presence of water (which has a similar H–O bond length) or the substitution of H into ND_4 would result in a decrease in the peak area.

We can see that the coordination number of Al has increased in the ammonium-exchanged sample to 4.23(3) (Table 4). This is in a reasonably good agreement with a calculation from NMR, where the average coordination number for NH_4^+-Y zeolites is 4.19.

This indicates that using local probes such as NMR and PDF analysis we can observe framework modification starting to occur in the structure after ammonium exchange.

3.4 TEM data

Finally, to be able to see if exchange has any effect on the morphology of the crystallites, we have performed TEM on samples 1 and 3 (Fig. 7 and 8). These figures demonstrate that the predominant sizes of the particles of both compounds are approximately similar and are around 0.6–1 micron. It can also be seen that both compounds produce particles with defined crystalline edges, seen as projections in the images. Some well defined symmetrical shapes can be seen for Na-Y particles (Fig. 7). For the Na-Y particles the predominant angles between the edges are 90 and 120 degrees, while for the ammonium-Y particles the predominant angles seem to be sharper, equal to 90 degrees or smaller in some cases. However, overall shapes of

Table 4 PDF analysis data: peak position, peak width and coordination number (CN) for Si, N and Al in the NH_4-Y sample determined from neutron diffraction data

Correlation	Peak position (Å)	Peak width (Å)	CN
N–D	1.028(1)	0.049(1)	1.24(1)
Si–O	1.620(1)	0.051(1)	4.00
Al–O	1.749(1)	0.089(1)	4.23(3)

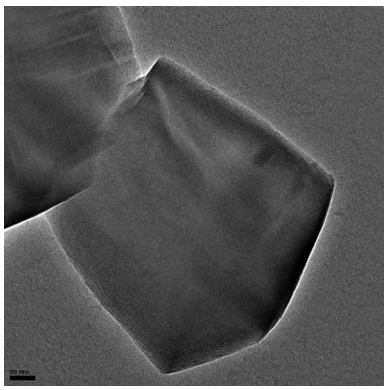

Fig. 7 TEM image of individual particles of Na-Y zeolite (sample 1) at 25 K magnification. Bar represents 50 nm.

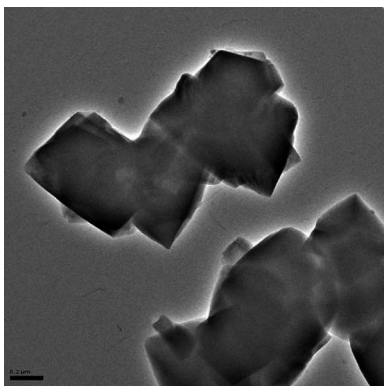

Fig. 8 TEM image of ammonium exchanged zeolite Y particles at 8 K magnification. Bar represents 0.2 μm.

particles are almost the same, we did not observe big differences between those two samples.

4 Discussion

The appearance of the octahedral peak around 0 ppm has been reported previously, but usually after calcination (above 400 °C), hydration of previously ammonium-exchanged zeolite, steaming and acid treatment.[11,13,16,17,22–24] Klinowski *et al.* reported the appearance of a strong peak around 0 ppm in the samples which were calcined and treated with acids.[11] Xu *et al.* reported similar occurrence of the peak around 0 ppm in samples which were calcined at 823 K.[24] As far as we know, there have been no reports of the appearance of an octahedral peak after ammonium exchange alone in zeolite Y.

To see if such disruption of the framework is unique to zeolite Y, we have synthesized Na zeolite A (with LTA framework) and have performed a similar "mild" exchange with ammonium (see ESI† for details of synthesis and exchange). The ^{29}Si NMR results for Na-A (sample 1a) and exchanged zeolite A (sample 1a) are presented in ESI.† Deconvolution of ^{29}Si NMR spectra gives a Si/Al ratio of 1.57 for Na-A and 1.6 for NH_4-A (using eqn (4)). The ^{27}Al NMR spectrum of the parent Na-A shows one peak at 58.64 ppm, corresponding to

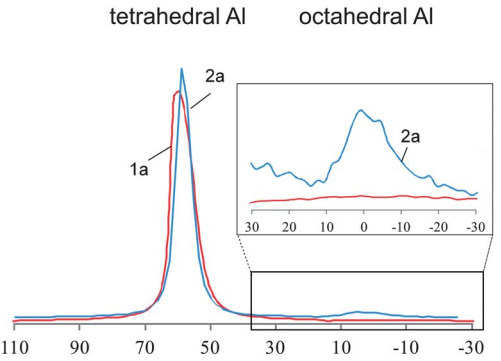

Fig. 9 High-resolution ^{27}Al MAS SS NMR spectrum for sample 1a (zeolite A) in red and sample 2a (NH_4-A zeolite) in blue, collected at 104.198 MHz. Peak centered at 58.64 ppm corresponds to tetrahedral aluminiums for zeolite Na-A. Peak centered at 56.63 ppm corresponds to tetrahedral Al and peak at −0.86 ppm corresponds to the appearance of octahedral Al in NH_4-A zeolite.

tetrahedral aluminium (Fig. 9), while an ^{27}Al NMR spectrum of the exchanged zeolite A has two resonances at 56.63 ppm and −0.86 ppm, corresponding to tetrahedral and octahedral species respectively. The ratio r of the intensities of the tetrahedral and the octahedral signals is 4.5. Thus we can recalculate the Si/Al $= 1.57(1 + r)/r = 1.91$ for the tetrahedral framework only. As, in the case with zeolite Y, this value is higher than 1.6 originally calculated from the ^{29}Si spectra. This confirms that exchange of sodium with ammonium in zeolites already leads to changes in the aluminium environment and disruption of the framework. In this case up to 5% of aluminium was displaced from tetrahedral to octahedral environments. The results of Na-A and exchanged zeolite A suggest that such aluminium migration is a common feature in zeolites.

It is not surprising that the average structure does not show disruption of the framework in zeolites, both diffraction patterns in Fig. 1 appear to be almost similar and show high crystallinity for both Na-Y and NH_4^+-Y zeolites, and there is a similar result from the average structure for zeolite A. It is possible however to detect the disruption of the framework and the change in aluminium environments by local probes, NMR and PDF analysis.

5 Conclusions

We have presented data for Na-Y and NH_4^+-Y zeolites using multiple experimental techniques. We show that exchange of NH_4^+ for Na^+ introduces local changes in the molecular framework of the zeolites by increasing the coordination number of Al species and displacing tetrahedral aluminium species to octahedral environments. These changes are directly observable by the use of local probes including NMR and PDF analysis. Formation of octahedral Al species is typically reported after calcination or other harsh treatment (high temperatures above 400 °C, steaming, acid treatment) of ammonium-exchanged frameworks; we have shown that the ammonium exchange itself introduces the octahedral Al species during the exchange. A similar result is obtained on Na-A zeolite which was exchanged with NH_4^+.

Acknowledgements

We thank Dr K. Borisenko and Dr G. Li (Department of Materials, Oxford) for collecting the TEM data and Dr S.A. Wells for useful discussions. We thank the Rutherford-Appleton Laboratory (Chilton, Oxfordshire, UK) for the use of ISIS facility. AS thanks the Royal Society (University Research Fellowship) for funding and Linacre College, Oxford, for Lucy Halsall Grant. We thank two anonymous reviewers for helpful comments.

References

1 D. Breck, *Zeolite Molecular Sieves*, Krieger, Malabar, FL, 1984.
2 J. Weitkamp and L. Puppe, *Catalysis and zeolites, fundamentals and applications*, Springer-Verlag, Berlin, 1999.
3 J. Cejka, H. V. Bekkum, A. Corma and F. Schuth, *Introduction to zeolite science and practice*, Elsevier, Amsterdam, 2007.
4 S. Kulprathipanja, *Zeolites in industrial separation and catalysis*, Wiley-VNC, Great Britain, 1st edn, 2010.
5 C. Baerlocher, W. Meier and D. Olson, *Atlas of zeolite framework types*, Elsevier, Amsterdam, 2001.
6 A. Sartbaeva, S. Wells, M. Treacy and M. Thorpe, *Nat. Mater.*, 2006, **5**, 962–965.
7 A. Sartbaeva, G. Gatta and S. A. Wells, *Europhys. Lett.*, 2008, **83**, 26002.
8 A. Sartbaeva, J. Haines, O. Cambon, M. Santoro, F. Gorelli, C. Levelut, G. Garbarino and S. A. Wells, *Phys. Rev. Lett.*, 2012, **85**, 064109.
9 S. A. Wells, A. Sartbaeva and G. Gatta, *Europhys. Lett.*, 2011, **94**, 56001.
10 E. Lippmaa, M. Magi, A. Samoson, G. Engelhardt and A.-R. Grimmer, *J. Am. Chem. Soc.*, 1980, **102**, 4889–4893.
11 J. Klinowski, J. Thomas, C. Fyfe and G. Gobbi, *Nature*, 1982, **296**, 533–536.
12 J. Klinowski, *Anal. Chim. Acta*, 1993, **283**, 929–965.
13 E. Bourgeat-Lami, P. Massiani, F. Direnzo, F. Espiau and T. Courieres, *Appl. Catal.*, 1991, **72**, 139–152.
14 M. Geppi, S. Borsacchi, G. Mollica and C. Veracini, *Appl. Spectrosc. Rev.*, 2009, **44**, 1–89.
15 W. Jacobs, J. de Haan, L. van de Ven and R. van Santen, *J. Phys. Chem.*, 1993, **97**, 10394–10402.
16 W. Lutz, H. Toufar, D. Heidemann, N. Salman, C. Ruscher, T. Gesing, J.-C. Buhl and R. Bertram, *Microporous Mesoporous Mater.*, 2007, **104**, 171–178.
17 G. Agostini, C. Lamberti, L. Palin, M. Milanesio, N. Danilina, B. Xu, M. Janousch and J. van Bokhoven, *J. Am. Chem. Soc.*, 2010, **132**, 667–678.
18 S. Ramdas, J. Thomas, J. Klinowski, C. Fyfe and J. Hartman, *Nature*, 1981, **292**, 228–230.
19 S. Ramdas and J. Klinowski, *Nature*, 1984, **308**, 521–523.
20 A. Gola, B. Rebours, E. Milazzo, J. Lynch, E. Benazzi, S. Lacombe, L. Delevoye and C. Fernandez, *Microporous Mesoporous Mater.*, 2000, **40**, 73–83.
21 J. Jiao, S. Altwasser, W. Wang, J. Weitkamp and M. Hunger, *J. Phys. Chem. B*, 2004, **108**, 14305–14310.
22 B. Wouters, T.-H. Chen and P. Grobet, *J. Am. Chem. Soc.*, 1998, **120**, 11419–11425.
23 B. Xu, F. Rotunno, S. Bordiga, R. Prins and J. van Brokhoven, *J. Catal.*, 2006, **241**, 66–73.
24 B. Xu, S. Bordiga, R. Prins and J. van Brokhoven, *Appl. Catal., A*, 2007, **333**, 245–253.
25 D. Ginter, A. Bell and C. Radker, *Molecular Sieves*, Van Norstrand Reinhold, New York, 1992.
26 T. Holland and S. Redfern, *J. Appl. Crystallogr.*, 1997, **30**, 84.
27 W. Baur, *Am. Mineral.*, 1964, **49**, 697–704.
28 J. Hrilijac, M. Eddy, A. Cheetham, J. Donohue and G. Ray, *J. Solid State Chem.*, 1993, **106**, 66–72.
29 W. Lim, S. Seo, G. Kim, H. Lee and K. Seff, *J. Phys. Chem. C*, 2007, **111**, 18294–18306.
30 A. Hannon, *Nucl. Instrum. Methods Phys. Res., Sect. A*, 2005, **551**, 88–107.
31 T. Egami and S. Billinge, *Underneath the Bragg peaks: structural analysis of complex materials*, Pergamon Press, Elsevier, Oxford, England, 2003.
32 P. Mitchell, S. Parker, A. Ramirez-Cuesta and J. Tomkinson, *Vibrational Spectroscopy with Neutrons with Applications in Chemistry, Biology, Materials Science and Catalysis*, World Scientific, 1st edn, 2005, vol. 3.
33 A. Ramirez-Cuesta, P. Mitchell, D. Ross, P. Georgiev, P. Anderson, H. Langmi and D. Book, *J. Alloys Compd.*, 2007, **446**, 393–396.
34 A. Ramirez-Cuesta, P. Mitchell, D. Ross, P. Georgiev, P. Anderson, H. Langmi and D. Book, *J. Mater. Chem.*, 2007, **17**, 2533–2539.
35 B. Hudson, *Vib. Spectrosc.*, 2006, **42**, 25–32.
36 W. Jacobs, R. van Santen and H. Jobic, *J. Chem. Soc., Faraday Trans.*, 1994, **90**, 1191–1196.
37 A. Sartbaeva, M. S. S. A. Wells, M. Lodge, M. Jones, A. Ramirez-Cuesta, G. Li and P. Edwards, *J. Cluster Sci.*, 2010, **21**, 543–549.
38 A. Seel, A. Sartbaeva, A. Ramirez-Cuesta and P. Edwards, *Phys. Chem. Chem. Phys.*, 2010, **12**, 9661–9666.
39 A. Seel, A. Sartbaeva, J. Mayers, A. Ramirez-Cuesta and P. Edwards, *J. Chem. Phys.*, 2011, **134**, 114511.
40 L. Kocheleva, *Russ. Chem. Bull.*, 1994, **43**, 346–350.